# Normal Shock Vortex Interaction

**O. Thomer, W. Schröder, and E. Krause**

Aerodynamisches Institut, RWTH Aachen
Wüllnerstraße zw. 5 und 7, 52062 Aachen, Germany
E-mail: oliver@aia.rwth-aachen.de

**Key words:** Supersonic Vortex Breakdown, Shock-Vortex Interaction, Longitudinal Supersonic Vortex, Euler- and Navier-Stokes Solutions

**Abstract:** *Breakdown of a slender longitudinal vortex caused by a normal shock is studied with a numerical solution of the* EULER *and the* NAVIER-STOKES *equations for time-dependent, three-dimensional, supersonic flow at a free stream* MACH *number of 1.6 and different vortex strengths. When breakdown occurs, a free stagnation point is formed downstream from the shock, followed by a region of reversed flow with a bubble-like flow structure. The burst part of the vortex grows in the axial and radial directions until the bubble reaches a stable position. The shock remains normal near the axis of the vortex but is curved further away from it. The flow downstream from the shock is slightly oscillating. The numerical results clearly reveal the time-dependent flow structure in the axial and the radial direction. The results compare well with recent experimental findings.*

## 1 Introduction

In continuation of previous studies [1, 2, 3, 4] the interaction of a longitudinal BURGERS vortex with a wake-like axial velocity profile and a normal shock is investigated for viscous supersonic flow at a MACH number of Ma=1.6. Such an interaction is encountered, for example, on strake-wing configurations at moderate and high angles of attack and compressors operating near their stability limits [5], where the tip vortex of the blades interacts with a normal shock during the passage through the compressor cascade. Although the breakdown process is mainly dominated by pressure forces, the flow inside the burst part of the vortex is also strongly influenced by viscous forces. A comparison of results of previous computations for inviscid flows with those for viscous flows presented here clearly exhibits that the vortex structures encountered in viscous flows inside the bubble are smaller, and that the bubble itself is smaller in its radial and axial extent.

## 2 Governing equations, boundary conditions, and computational domain

The numerical solution used in the present analysis is based on the EULER and the NAVIER-STOKES equations for time-dependent, three-dimensional, compressible flow. The convective terms are discretized with an explicit finite-volume scheme based on the $AUSM+$ approach by LIOU [6]. The dissipative terms, including the STOKES stresses and the FOURIER heat flux vector, are discretized using an adapted cell-vertex scheme, and the time-derivatives are approximated via a 5-step RUNGE-KUTTA scheme. Details of the computational method are presented in [2]. The computational domain is a rectangular box with 99x99x199 grid points in the $x$-$y$-, and $z$-direction (Fig. 1). Near the axis of the vortex the grid is clustered so that the vortex core ($r < 1$) is resolved with approx. 21 grid points in the radial direction. The inflow and initial conditions are prescribed with a slender BURGERS vortex in dimensionless form

$$v_\varphi(r) = \frac{\Gamma_0 \cdot r}{2\pi} \cdot e^{\frac{1-r^2}{2}} \quad ; \quad v_z(r) = v_{z_\infty} \cdot (1 - \delta \cdot e^{-\mu_w \cdot r^2}) \quad ; \quad v_r(r) = 0 \tag{1}$$

*Paper presented at the RTO AVT Symposium on "Advanced Flow Management: Part A – Vortex Flows and High Angle of Attack for Military Vehicles", held in Loen, Norway, 7-11 May 2001, and published in RTO MP-069(I).*

# Report Documentation Page

*Form Approved*
*OMB No. 0704-0188*

Public reporting burden for the collection of information is estimated to average 1 hour per response, including the time for reviewing instructions, searching existing data sources, gathering and maintaining the data needed, and completing and reviewing the collection of information. Send comments regarding this burden estimate or any other aspect of this collection of information, including suggestions for reducing this burden, to Washington Headquarters Services, Directorate for Information Operations and Reports, 1215 Jefferson Davis Highway, Suite 1204, Arlington VA 22202-4302. Respondents should be aware that notwithstanding any other provision of law, no person shall be subject to a penalty for failing to comply with a collection of information if it does not display a currently valid OMB control number.

| | | |
|---|---|---|
| 1. REPORT DATE<br>**00 MAR 2003** | 2. REPORT TYPE<br>**N/A** | 3. DATES COVERED<br>**-** |

| | |
|---|---|
| 4. TITLE AND SUBTITLE<br>**Normal Shock Vortex Interaction** | 5a. CONTRACT NUMBER |
| | 5b. GRANT NUMBER |
| | 5c. PROGRAM ELEMENT NUMBER |
| 6. AUTHOR(S) | 5d. PROJECT NUMBER |
| | 5e. TASK NUMBER |
| | 5f. WORK UNIT NUMBER |
| 7. PERFORMING ORGANIZATION NAME(S) AND ADDRESS(ES)<br>**NATO Research and Technology Organisation BP 25, 7 Rue Ancelle, F-92201 Neuilly-Sue-Seine Cedex, France** | 8. PERFORMING ORGANIZATION REPORT NUMBER |
| 9. SPONSORING/MONITORING AGENCY NAME(S) AND ADDRESS(ES) | 10. SPONSOR/MONITOR’S ACRONYM(S) |
| | 11. SPONSOR/MONITOR’S REPORT NUMBER(S) |

12. DISTRIBUTION/AVAILABILITY STATEMENT
**Approved for public release, distribution unlimited**

13. SUPPLEMENTARY NOTES
**Also see: ADM001490, Presented at RTO Applied Vehicle Technology Panel (AVT) Symposium held inLeon, Norway on 7-11 May 2001, The original document contains color images.**

14. ABSTRACT

15. SUBJECT TERMS

| 16. SECURITY CLASSIFICATION OF: | | | 17. LIMITATION OF ABSTRACT | 18. NUMBER OF PAGES | 19a. NAME OF RESPONSIBLE PERSON |
|---|---|---|---|---|---|
| a. REPORT<br>**unclassified** | b. ABSTRACT<br>**unclassified** | c. THIS PAGE<br>**unclassified** | **UU** | **12** | |

**Standard Form 298 (Rev. 8-98)**
Prescribed by ANSI Std Z39-18

In the above equation $v_\varphi(r)$ is the circumferential, $v_z(r)$ the axial, and $v_r(r)$ the initial radial velocity component. Figure 2 shows the vortex parameters as a function of the core radius at a free stream MACH number of $Ma_\infty$=1.6. The quantity $\Gamma_0 = \Gamma_0^*/(a_0^* \cdot r_0^*)$ is the circulation of the vortex scaled with the speed of sound at stagnation conditions, $a_0^*$ and the radius of the vortex core $r_0^*$ at $r = r^*/r_0^*$=1. The quantity $\delta$=0.1 determines a wake-like axial velocity profile, and $r = \pm\sqrt{1/(2\mu_w)}$ describes the position of the point of inflection for $\mu = 1$. The initial radial pressure distribution is obtained by solving the radial momentum equation for slender vortices; the temperature is computed by assuming constant stagnation enthalpy for the radial direction, and the equation of state yields the density. For the subsonic part of the outflow plane (Fig. 1, plane 6) a non-reflecting boundary condition based on the characteristic approach by POINSOT & LELE [7] for viscous flows is chosen. The shock is prescribed by the RANKINE-HUGONIOT relations in the $x$-$y$ plane at $z$=0. The remaining horizontal and vertical boundaries of the computational domain (Fig. 1, plane 1 to 4) are represented by stream surfaces, so that the kinematic flow condition holds. The computation was initialized by prescribing the shock in the middle of the computational domain. The main flow is in the $z$-direction. Upstream of the shock the slender vortex is embedded in the main flow whereas downstream a uniform flow is specified.

# 3 Results

It was shown in [2], that normal-shock vortex-interaction does not necessarily lead to vortex breakdown. In fact, when the vortex strengths, e.g. its circulation, is small, the vortex can pass the shock without generally changing its shape. Two major statements could be made: First, by passing the shock the axial velocity profile of the vortex, which was uniform upstream of the shock, becomes wake like. The deceleration of flow has its maximum on the vortex axis. Second, the vortex circumferential velocity component remained nearly unchanged when passing the shock. The first can be explained by the pressure minimum on the vortex axis, the second finding agrees with the shock relations. These observations were also made by DELERY [10] in his experiments.

Increase of the vortex strengths, say the circumferential velocity, or the shock strength through the free stream MACH number, or the vortex deficit of the axial flow the interaction with the normal shock leads to vortex breakdown. This can be seen in Figure 3. The left column shows the MACH number distribution and the right column shows the streamlines in the symmetry $x$-$z$-plane of the computational domain for various vortex strengths of $\Gamma_0$=3.5, 4.0, 4.5. The instantaneous pictures of the EULER computations show that at vortex breakdown a free stagnation point on the vortex axis is formed. The shock is curved forward and a bubble-like flow regime grows in the lateral and axial directions until a nearly stable, slightly oscillating shock topology is reached. Inside the breakdown bubble counter-clockwise rotating ring-like vortical structures are generated, so that the stagnation point on the vortex axis is stabilized by the backflow caused by the ring-like vortical structures perpendicular to the vortex axis. By either increasing the vortex strength, the free stream MACH number or the vortex deflection parameter $\delta$ the interaction of the comprehensive effects lead to strong vortex breakdown.

Figure 4 shows the breakdown caused by the normal-shock vortex-interaction at $Ma_\infty$=1.6, $\Gamma_0$=5.0, for a time level $t$=200 for inviscid (left column) and viscous flow computation ($Re$=15000, right column). The upper pictures the three-dimensional vorticity distribution at strong vortex breakdown can be seen. In these pictures the MACH number distribution of the $x$-$z$ symmetry plane of the computational domain is projected to the boundary surface of the computational domain. It can be seen that the inviscid flow computation (left column) yields vortical structures larger than those of the viscous computation. The MACH number and pressure contours confirm a multiple shock structure (Fig. 4 b). The deformed shock resembles that of a bow shock observed at supersonic flow around blunt bodies. Further away from the axis the shock angle decreases until a shock-shock interaction is encountered. The calculation for inviscid flow yields two adjacent counterclockwise rotating vortex rings in the bubble. For the viscous computations multiple vortex structures can be observed inside the bubble. An analysis of the time-development of the flow shows a periodic shedding of the vortex rings. A detailed investigation of the flow pattern evidences that the two vortices are separated by a shock which is caused by a supersonic jet like flow in the upstream direction along the axis (Figure 6). This shock is perpendicular to the axis of symmetry. The streamlines in the recirculation zone show a convergent-divergent nozzle-like flow structure that enables the flow to be supersonic again inside the bubble. The acceleration to supersonic flow inside the bubble was already noticed by ERLEBACHER ET. AL. in their numerical investigations [9].

In the lower part of Figure 4 the MACH number distribution in a plane perpendicular to the vortex axis is shown. A fan like flow regime with multiple shock structures can be observed which also was noticed by BRILLANT ET. AL. in their experiments [12].

Figure 5 shows a time sequence from $t{=}r_0^*/a_0^*{=}60$ to $t{=}200$. The instantaneous pictures in the two columns left show the projections of the streamlines and the vortex lines $dz/dx = \omega_z/\omega_x$ in the horizontal center plane $y{=}$const. (see Fig. 1) of the domain of integration. The third column represents a sequence of $\lambda_2$-surfaces, that to a certain extent can be identified with surfaces of constant pressure [8], and in color of the local density. In the fourth column the pressure, density, temperature, MACH number $Ma_z$, and velocity $w$ component in the z-direction along the axis of the vortex are shown. The pictures clearly indicate that with increasing time a free stagnation point on or near the axis is formed, followed by a bubble-like flow structure. The bubble grows in the lateral and axial directions in time, until a stable, only slightly oscillating state is reached. Inside the bubble several small ring-like vortex structures can be identified, traveling downstream with progressing time. From the velocity and MACH number distributions it can be seen that there is a strong axial reverse flow along the axis of the vortex. The $\lambda_2$-surface representations confirm the ring-like structures inside the bubble. For increasing time the flow deviates more and more from its initial axial symmetry, confirming that it can be concluded that vortex breakdown is a truly three-dimensional process which cannot be described using a formulation for axially symmetric flows.

The schlieren picture in Fig. 7, shows the bubble topology of the computation. In the parallel experimental investigations the vortex is produced with a double wedge airfoil in a supersonic flow. When vortex breakdown occurs, the shock is deformed upstream, and the characteristic length scale of the arising bubble is of the order of the diameter of the core of the impinging vortex.

In addition to the numerical and experimental investigations, a breakdown criterion was derived for uniform axial flow (Fig. 8). Based on the axial momentum equation for inviscid flow and the RANKINE-HUGONIOT relations, the onset of breakdown can be predicted by requiring a stagnation point to be formed on the axis. In reference [2] it is shown that a breakdown condition based on the momentum equation along the vortex axis reads

$$\underbrace{\frac{p^*_{1_{AXIS}}}{p^*_{1_\infty}}}_{I} + \underbrace{\frac{\rho^*_{1_{AXIS}} \cdot v^{2*}_{z1_{AXIS}}}{p^*_{1_\infty}}}_{II} \geq \underbrace{\frac{p^*_{2_\infty}}{p^*_{1_\infty}}}_{III} \quad . \tag{2}$$

In the above equation, the pressure and momentum forces are written with respect to the free stream pressure $p^*_{1_\infty}$. In the case of uniform axial flow, the second term (II) on the left side can be written in the following form

$$\frac{\rho^*_{1_{AXIS}} \cdot v^{2*}_{z1_{AXIS}}}{p^*_{1_\infty}} = \gamma \cdot \frac{\rho^*_{1_{AXIS}}}{\rho^*_{1_\infty}} \cdot Ma^2_{1_\infty} \quad . \tag{3}$$

Since CROCCOS equation

$$T\nabla s + \vec{v} \times (\nabla \times \vec{v}) = \frac{\partial \vec{v}}{\partial t} + \nabla h_0 \tag{4}$$

yields $T \cdot \nabla s = \nabla h_0$ if the velocity and the vorticity vector are parallel to each other in steady flows the radial momentum equation for slender vortices

$$\frac{\partial p^*}{\partial r^*} = \frac{\rho^* v^{2*}_\varphi}{r^*} \tag{5}$$

can be solved for the velocity distribution given by equation (1). Together with the Rankine Hugoniot relation for the pressure ratio across a normal shock (term III)

$$\frac{p_2^*}{p_1^*} = 1 + \frac{2 \cdot \gamma}{\gamma + 1}(Ma_\infty^2 - 1) \quad , \tag{6}$$

the axial momentum equation (2) leads to the following breakdown criterion

$$\underbrace{(1 - \frac{(\gamma-1)\cdot\Gamma_0^2\cdot e^1}{16\pi^2[2+(\gamma-1)Ma_\infty^2]^{-1}})^{\frac{\gamma}{\gamma-1}}}_{p^*_{1_{AXIS}}/p^*_{1_\infty}} + \underbrace{\frac{\gamma Ma_{1_\infty}^2}{(1 - \frac{(\gamma-1)\Gamma_0^2\cdot e^1}{16\pi^2[2+(\gamma-1)Ma_\infty^2]^{-1}})^{\frac{-1}{\gamma-1}}}}_{\rho^*_{1_{AXIS}}/\rho^*_{1_\infty}} \geq \underbrace{1 + \frac{2\gamma}{\gamma+1}(Ma_\infty^2 - 1)}_{p^*_{2_\infty}/p^*_{1_\infty}} \quad . \tag{7}$$

From the above equation the circulation $\Gamma_0$ for which breakdown occurs can be determined. The corresponding spiral angle $\tau$ is defined by the quotient of the circumferential and the axial velocity

$$\tau = \frac{v_\varphi^*(r^* = r_0^*)}{v_z^*(r^* = r_0^*)} = \frac{\Gamma_0 \cdot \sqrt{1 + \frac{\gamma-1}{2}Ma_\infty^2}}{2\cdot\pi\cdot Ma_\infty \cdot (1 - \delta \cdot e^{-\mu_w})} \tag{8}$$

as a function of the free stream MACH number $Ma_\infty$. The comparison of the results obtained using the above relation with theoretical, numerical and experimental data [9, 10, 11] shows good agreement in the range of $1.5 \leq Ma_\infty \leq 2.0$ (Fig. 9).

# 4 Concluding Remarks

Breakdown of longitudinal slender vortices in supersonic flow, caused by the interaction with a normal shock, was investigated using a numerical solutions of the EULER and NAVIER-STOKES equations. The investigation of the normal shock-vortex interaction yields two types of flow fields downstream from the shock. Depending on the inflow parameters a weak interaction with no vortex breakdown was observed, and a strong interaction with a bubble-like vortex breakdown. The calculations show, that a slender vortex propagating across a normal shock does not necessarily leads to breakdown. If the circulation of the vortex is small and if the axial velocity profile is uniform, the vortex does not change its overall shape. By increasing the vortex strengths, the free stream MACH number or the vortex deflect of the axial flow the shock vortex interaction leads to a free stagnation point on or nearby the vortex axis, which can be understood as the initialization of vortex breakdown. The results obtained indicate, that the flow structure of the burst part of the vortex as simulated with the numerical solution agrees well with experimental observations. Several ring-like, slightly oscillating vortex structures are formed immediately downstream from a stagnation point on the axis. For certain flow conditions strong upstream flow motion, even supersonic flow may occur near the axis. A breakdown criterion was derived that showed good agreement with numerical and experimental findings.

## Acknowledgements

This research is being supported by the Deutsche Forschungsgemeinschaft. The support is gratefully acknowledged. Mr. M. Klaas (Aerodynamisches Institut, RWTH-Aachen) provided the color schlieren picture.

*Addresses:* DIPL.-ING. O. THOMER, PROF. DR.-ING. W. SCHRÖDER, AND PROF. EM. E. KRAUSE, PH.D., Aerodynamisches Institut der RWTH Aachen, Wüllnerstr. zw. 5 u. 7, 52062 Aachen, Germany.

# 5 Figures

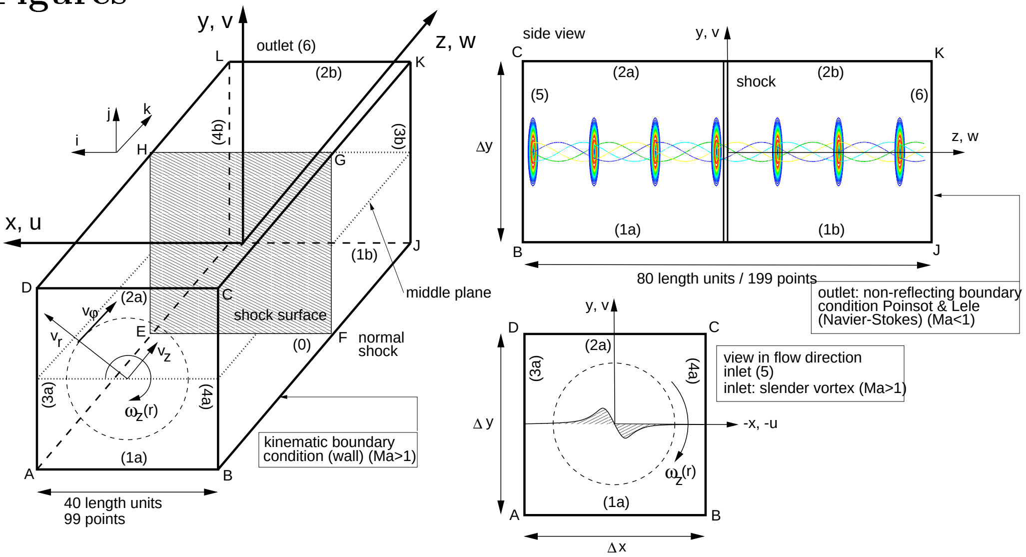


Figure 1: Computational setup and boundary conditions for normal shock-vortex interaction. Flow is in the positive $z$-direction.

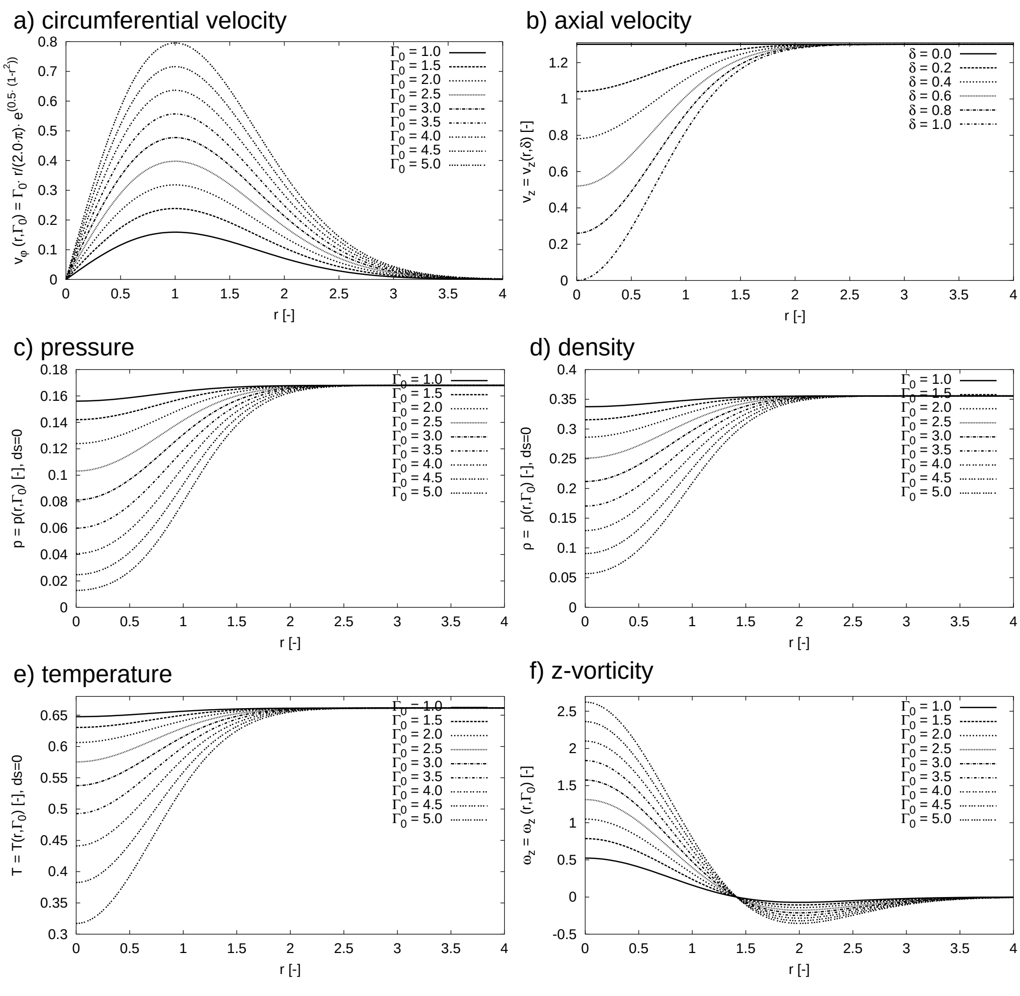


Figure 2: Vortex parameters as a function of $r$ at $Ma_\infty$=1.6, $\gamma$=1.4, $\Gamma_0$=1.0..5.0

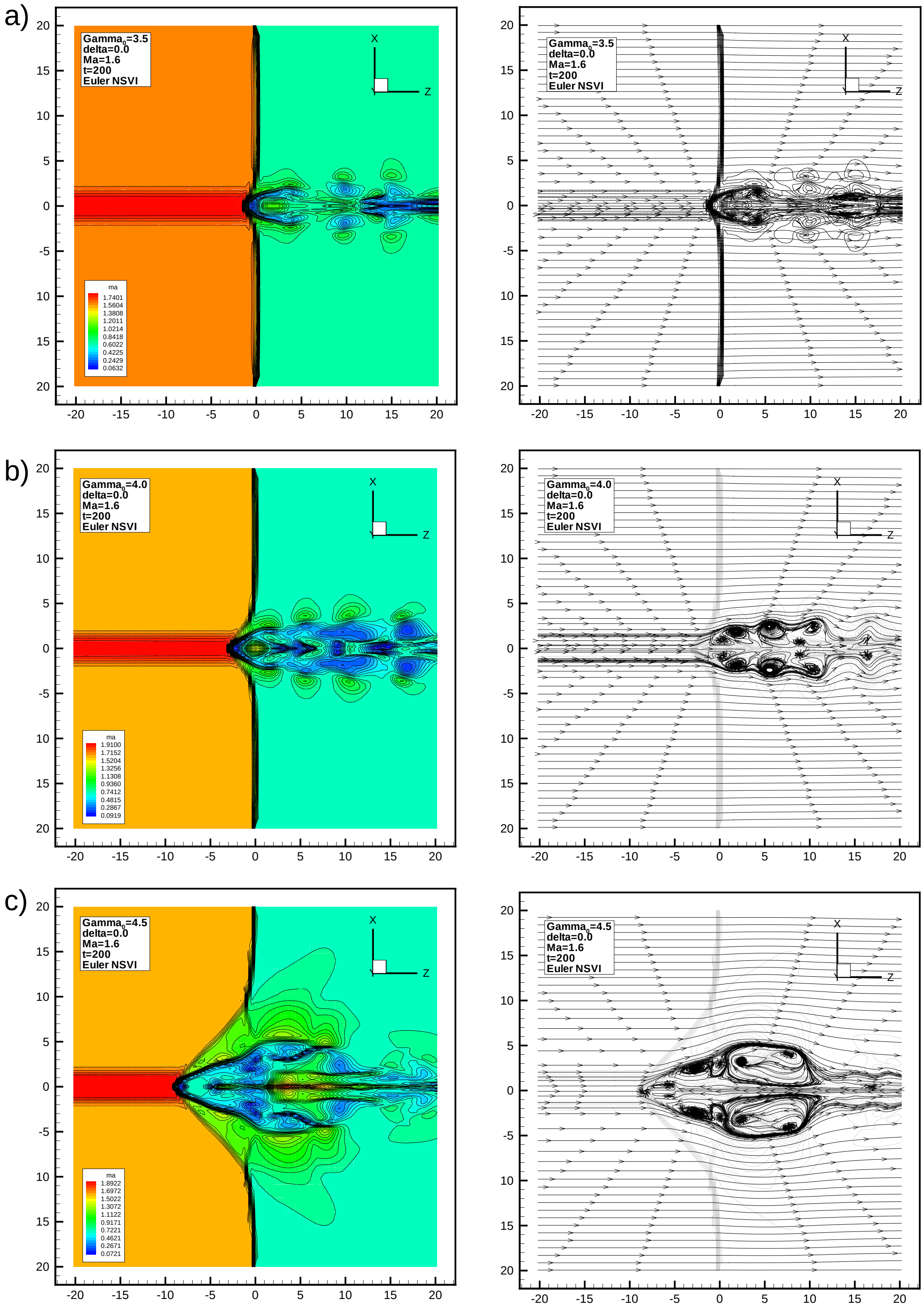


Figure 3: MACH number distribution (left column) and streamlines (right column) in the midplane of the computational domain at $Ma_\infty$=1.6, $\Gamma_0$=3.5, 4.0, 4.5, and inviscid, uniform flow (time step $t$=200).

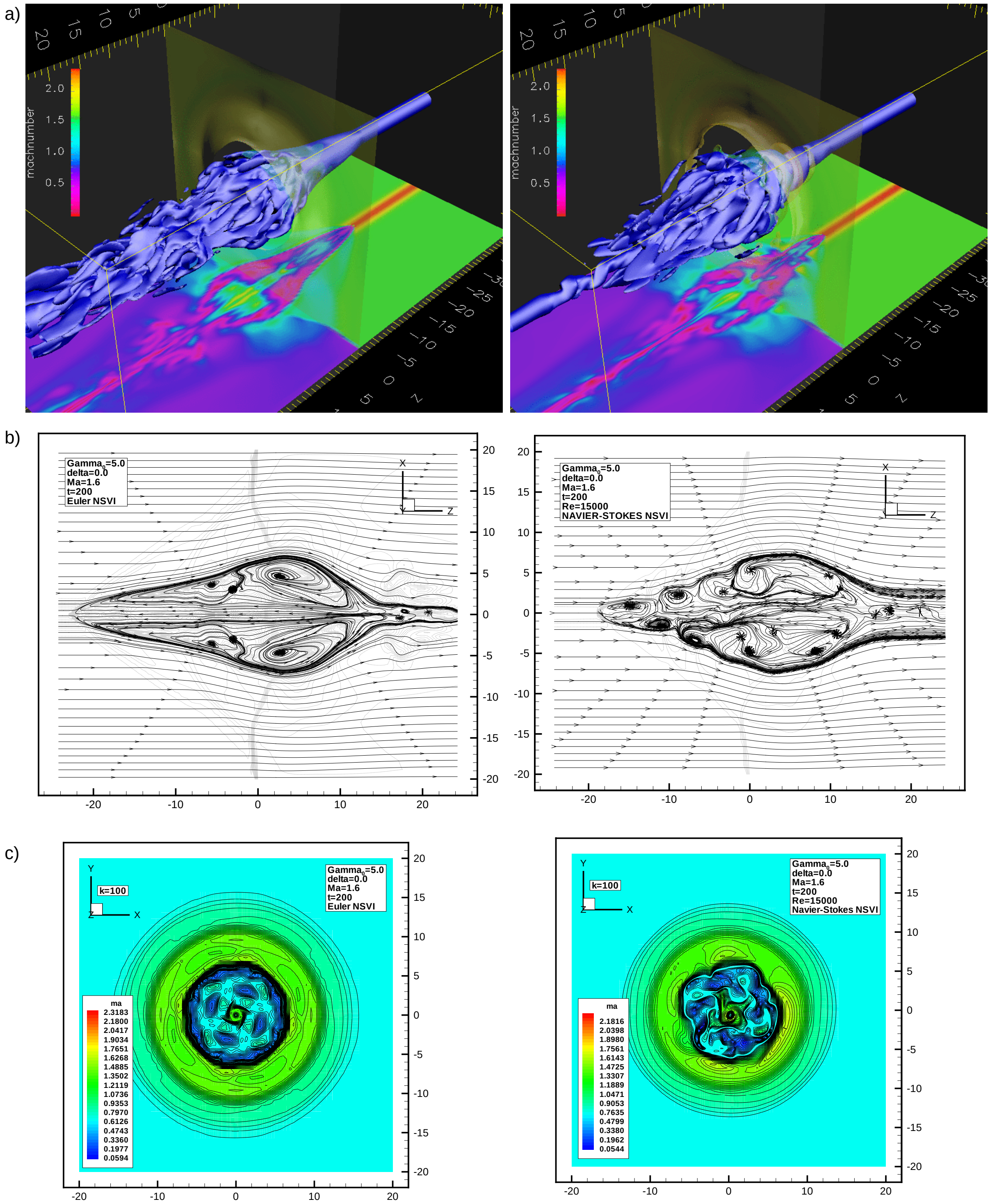


Figure 4: Instantaneous pictures at time step $t$=200 of the Euler (left column) and Navier-Stokes (right column) computations ($Ma_\infty$=1.6, $\Gamma_0$=5.0, and $\delta$=0). a) spatial iso-vorticity surface combined with the Mach number distribution projected on the lower boundary. b) streamline pattern in the $x$-$z$-middle plane of the bubble, and c) Mach number distribution within the bubble at the $x$-$y$-plane for $z = 0$.

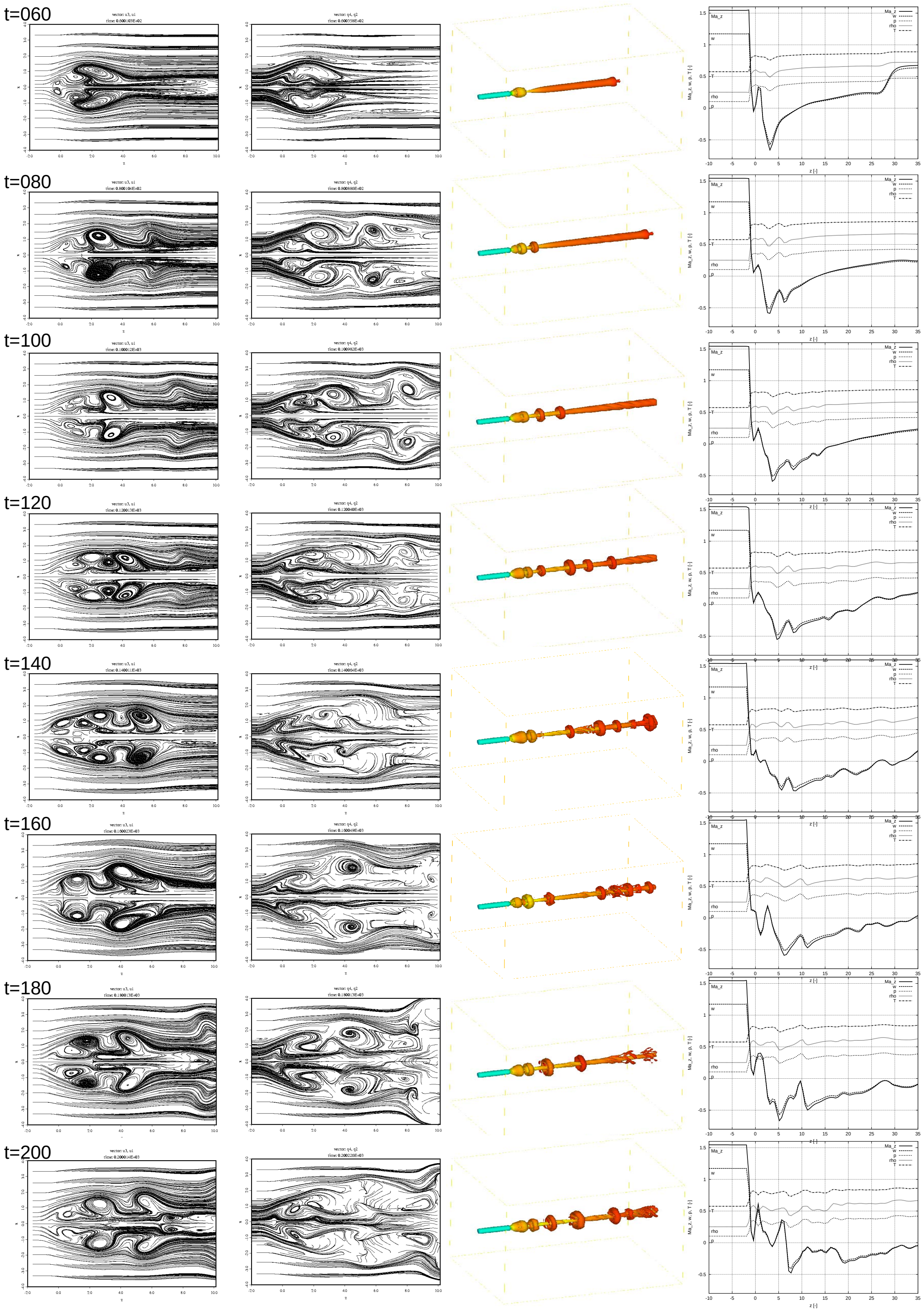


Figure 5: Evolution in time of streamlines (1st column), and vorticity contours (2nd column) in the center plane $y = 0$; $\lambda_2$-iso surface (3d column); distribution of the primitive variables and the MACH number on the centerline (4th column from left to right) for certain time steps for normal shock-vortex interaction ($Ma_\infty = 1.6$, $\Gamma_0 = 2.5$, $\delta = 0.1$).

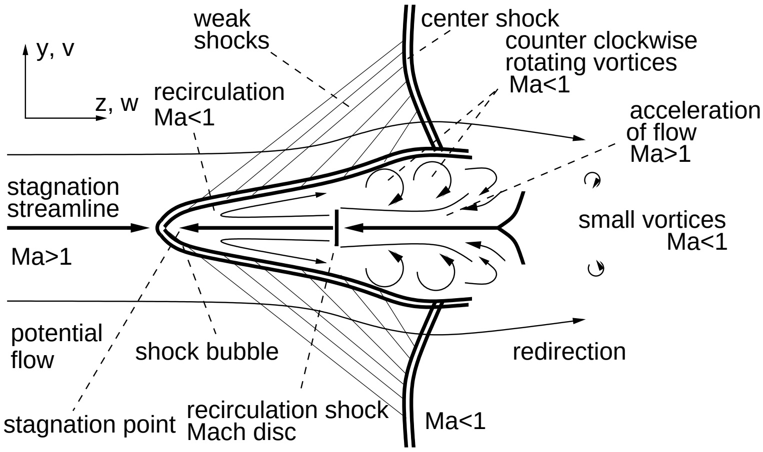


Figure 6: Flow schematic for strong vortex breakdown at time step $t = 200$.

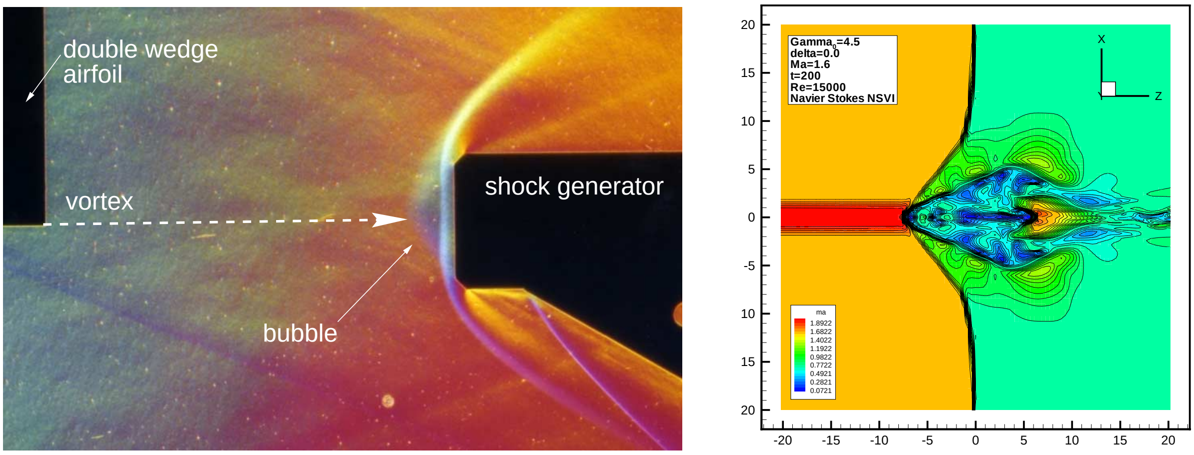


Figure 7: Color schlieren picture (M. Klaas, private communications) (left) and numerical MACH number distribution (right) at $Ma_\infty = 1.6$, $\Gamma_0$=4.5, $\delta$=0 for uniform axial flow at $Re$=15000. Flow is from left to right.

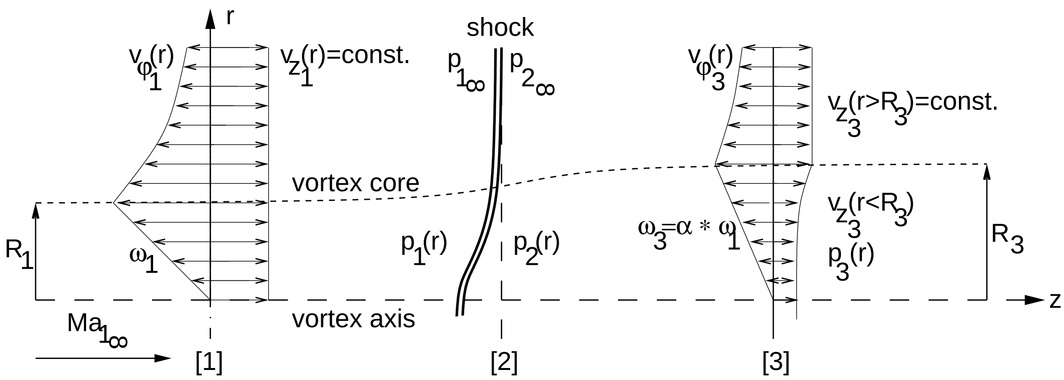


Figure 8: Theoretical model to predict vortex breakdown.

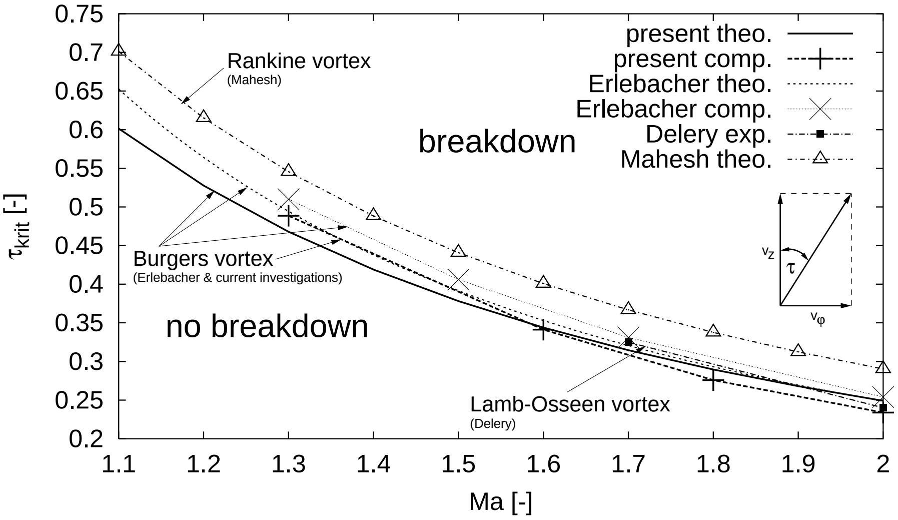


Figure 9: Breakdown map for normal-shock vortex-interaction.

# References


[1] O. Thomer, W. Schröder and M. Meinke, Numerical Simulation of Normal- and Oblique-Shock Vortex Interaction, ZAMM Band 80, Sub. 1, pp. 181-184, 2000.

[2] O. Thomer, E. Krause, W. Schröder and M. Meinke, Computational Study of Normal and Oblique Shock-Vortex Interactions, ECCOMAS 2000, Barcelona 11-14. September, 2000.

[3] O. Thomer, W. Schröder and E. Krause, Numerical and experimental investigations on the supersonic vortex breakdown phenomena, GAMM conference, Zürich 11-14. February, 2001.

[4] E. Krause, Shock Induced Vortex Breakdown, Invited paper presented at the 10th International Conference on Methods of Astrophysical Research, Novosibirsk, Russia, July 9-16, 2000.

[5] S. Schlechtriem and M. Lötzerich, Breakdown of tip leakage vortices in compressors at flow conditions close to stall, IGTI-ASME conference, Orlando Florida, 1997.

[6] M. S. Liou, A Sequel to AUSM: AUSM+, Journal of Computational Physics, vol. 129, pp. 164-382, 1996.

[7] T. J. Poinsot and S. K. Lele, Boundary Conditions for Direct Simulations of Compressible Viscous Flows, Journal of Computational Physics, vol. 101, pp. 104-129, 1992.

[8] J. Jeong and F. Hussain, On the identification of a vortex, J. Fluid Mech., vol. 285, pp. 69-94, 1995.

[9] G. Erlebacher , M. Y. Hussaini and C. W. Shu, Interaction of a Shock with a Longitudinal Vortex, ICASE Report, Vol. 198332, 1996.

[10] Jean M. Delery, Aspects of Vortex Breakdown, Prog. Aerospace Sci., vol. 30, pp. 1-59, 1994.

[11] K. Mahesh, A Model for the Onset of Breakdown in an Axisymmetric Compressible Vortex, Physical Fluids, pp. 3338-3345, vol. 8, no. 12, 1996.

[12] P. Brillant, J. M. Chomaz, P. Huerre et. al., Instabilities and vortex breakdown in swirling jets and wakes, IUTAM Symposium on Dynamics of Slender Vortices, Aachen, pp. 267-286, 1997.

**Paper: 18**
**Author: Mr. Thomer**

**Question by Mr. Jeune**: Concerning the vortex breakdown. limit presented as a function of Mach number for normal shock case, should it be possible to correlate this limit for both normal and oblique shocks by considering the pressure jump across the shock?

Answer: No, unfortunately not. In case of normal shocks the flow downstream of the pressure jump is subsonic. This is a “must” for the decelerated flow on the vortex axis in order to obtain a free stagnation point. In case of an oblique shock, not only must the pressure jump across the shock be a criterion, but also the “strong” shock solution must be obtained locally in the vicinity of the vortex core. Therefore, locally at vortex axis, a small subsonic pocket has to be formed in which the flow is decelerated so that a stagnation point becomes possible. By taking a look on the local Mach numbers, the water parameters $\delta$ can be varied to reduce the $M_{axis}$ such that $M_{axis} << M_{oo}$. The flow on the vortex axis is not able anymore to follow the redirection (given by the ramp angle) so that locally a normal shock is formed. If now, as a second criterion, the pressure jump across this locally normal shock is sufficient, the vortex will break down.

For further information about that, please take a look at my ECCOMAS paper 2000, listed in the references.

**This page has been deliberately left blank**

**Page intentionnellement blanche**